Carpathian Journal of Earth and Environmental Sciences, May 2015, Vol. 10, No. 2, p. 159 - 174

INTERACTION OF THE HILLSLOPES AND VALLEY BOTTOMS ON THE NW SLOPE OF THE LYSÁ HORA MT., THE HIGHEST PEAK OF THE WESTERN BESKIDS

Václav STACKE[1] & Petr TÁBOŘÍK[2]

[1]*Centre of Biology, Geoscience and Environmental Education, University of West Bohemia; Klatovská 51, Plzeň, Czech Republic, e-mail: vaclav@stacke.cz*

[2]*Institute of Hydrogeology, Engineering Geology and Applied Geophysics, Charles University in Prague; Albertov 6, Praha, e-mail: petr.taborik@post.cz*

Abstract: To reveal the slope-channel interaction in the highest parts of the Western Beskids, we studied the valley floor, colluvial accumulations and slope deformations in the Satina River valley (Outer Western Carpathians, Czech Republic). GNSS geomorphological mapping, geophysical sounding and detailed lithological analyses (grain-size, fabric, clast orientation and particle shape) of the valley infill enabled the presumable reconstruction of the processes that formed the valley. In the uppermost part of the valley the gradual change from the U-shaped to the V-shaped valley is distinctive. The river channel is vertically cut in the middle part of the valley (ca 19 m into the sediments and further 3 m into the bedrock formed by thinly laminated claystones). Colluvial layers formed by multigenerational debris flows with fluvial intercalations form the sedimentary infill in this stretch. The method of electrical resistivity tomography has confirmed deep-seated disintegration of the Lukšinec ridge and the occurrence of several generations of rockslides and rather shallow debris slides on the slopes above the studied site. Accumulations of the landslides are considered to be the source area of a large volume of colluvial sediments in the Satina river catchment. The alternations of layers of different genesis indicate high dynamics of the landscape development in the area. Particular debris flow events were separated by periods of prevailing fluvial processes. A part of the landslide area had been saturated and its consequent reactivation led to the formation of the new debris slide with shallow planar slip plane after the 1997 extreme rainfall event. The canyon-like valley incised into the sandstone flysch rocks is preserved in the lower parts of the catchment. The studied part of the catchment is thus characterized by the geomorphological processes pattern change observed in the formation of a large accumulation in transport limited conditions of a colder period of the Pleistocene (forest-free area) and intensive vertical cutting in supply limited conditions of the Holocene.

Keywords: sedimentology, debris flow, valley incision, electrical resistivity tomography

1. INTRODUCTION

The Western Carpathians are one of the most dynamic landscapes in the central Europe (e.g. Záruba, 1922; Krejčí et al., 2002; Smolková et al., 2008; Pánek et al., 2009; Stacke et al., 2014;). Its surface is intermittently shaped mainly by the various types of slope (Pánek et al., 2011; Šilhán et al., 2011; Šilhán, 2012b; Pánek et al., 2013b) and fluvial (Starkel et al., 2006; Škarpich et al., 2011; Pánek et al., 2013a) processes during Quaternary period. Mainly the Late Pleistocene and Holocene slope deformations (Alexandrowicz, 1993; Alexandrowicz & Alexandrowicz, 1999; Hradecký et al., 2004; Margielewski, 1997; Margielewski, 1998; Margielewski, 2001; Margielewski, 2003; Margielewski, 2006; Baroň, 2007; Hradecký et al., 2007; Smolková et al., 2008; Šilhán, 2012a; Pánek et al., 2013b) and alluvial fans (Šilhán & Stacke, 2011; Šilhán, 2014) were studied in last few decades, as well as the Holocene evolution of mountain (e.g. Kukulak, 2003; Škarpich et al., 2011; Pánek et al., 2013a) and the piedmont floodplains (e.g. Starkel, 1995; Starkel et al., 2006; Starkel et al., 2007; Stacke et al., 2014). The information on both landscape and environmental evolution can be traced within landslide accumulations (e.g. peatbogs, buried trunks) (e.g. Margielewski & Kovalyukh, 2003; Margielewski et al., 2010;

Margielewski et al., 2011), sedimentary traps (e.g. landslide dammed lakes) (Smolková et al., 2008; Smolková, 2011) and in mountainous and sub-mountainous fluvial archives in the floodplains (e.g. Coulthard & Macklin, 2001; Kalis et al., 2003; Macaire et al., 2006). The probability density curve of landslide events that occurred in Czech and Polish part of the Outer Western Carpathians during Late Pleistocene and Holocene was created based on information from some of abovementioned environments (Pánek et al., 2013b).

Several studies have been focused on the catchments of mountainous and sub-mountainous rivers in the Carpathians and their foreland. Detailed studies have been performed in the Eastern Carpathian rivers such as the Moldova (Chiriloaei et al., 2012) and Dniester (Huhmann & Brückner, 2002; Huhmann et al., 2004; Gębica et al., 2013), and in the Western Carpathians especially in the Belá (Kidová & Lehotský, 2012), San (Kukulak, 2003), Vistula (Kalicki et al., 1996; Kalicki, 2000) and Wisłoka (Starkel, 1995). As for the Carpathian foreland in the Czech Republic, detailed studies were performed in the Morávka (Škarpich et al., 2013) and in the Bečva River floodplains (Stacke et al., 2014) and in the lower part of the Morava river floodplain (Kadlec et al., 2009; Grygar et al., 2010; Bábek et al., 2011). In these fluvial archives, evidence of climatically induced palaeoenvironmental changes is well demonstrated especially for the Last Glacial/Holocene transition (e.g. Kalicki et al., 1996; Starkel et al., 2007) and for the Late Holocene neoglaciation (e.g. Huhmann et al., 2004; Starkel et al., 2006; Stacke et al., 2014).

Unlike the other Carpathian regions that were significantly affected by humans no later than during Roman Times (400 BC – 200 AD) (e.g. Tóth, 2001; Derwich & Żurek, 2002), the Outer Western Carpathians remained in semi-natural conditions with negligible human impact up to the 12th century, when the colonisation of the mountain piedmont took place (Opravil, 1974). Vast portions of the mountainous part of the region were nearly intact even up to the end of the 16th century when extensive deforestation interrelated with grazing activity (the so-called Wallachian colonisation) occurred (Kalicki, 2000; Gębica et al., 2013). Thus, the western part of the Carpathians was one of the last central European regions affected by humans.

The primary aims of our study are (i) to identify extent, thickness and architecture of the Satina River valley infill, (ii) to describe the impact of environmental changes on the slope – stream channel coupling and (iii) to reconstruct processes that formed the present landscape and fit them into the wider framework.

A multidisciplinary approach is necessary to understand the complexity of the spatio-temporal evolution of mountain slopes and its coupling with valley bottoms (e.g. Harvey, 2001; Brown et al., 2009; Keesstra et al., 2009; Pánek et al., 2011; Baroň et al., 2014). Therefore, geomorphological, geophysical and sedimentological analyses were used to form a complete explorative framework.

2. REGIONAL SETTINGS

The Satina river (Q_a = ~90 $l.s^{-1}$; catchment area = 7.4 km^2) is a mountainous river, the right tributary of the Ostravice River in the eastern part of the Czech Republic (Fig. 1). The river originates at an elevation 940-980 m a.s.l. on the NW slope of the Lysá hora Mt (1323 m a.s.l. - the highest peak of the Western Beskids Mts). The bedrock of the catchment is composed of the thin to thick-bedded flysch formed of Cretaceous and Paleogene calcareous claystone and sandstone of the Outer (Menilite-Krosno) Group of Nappes (Menčík et al., 1983). The highest parts of the catchment and the nearby ridges are built by nearly horizontally inclined (<10°) thick-bedded flysch of the Middle Godula Member; weak thin-bedded flysch of the Lower Godula Member rises in the middle and lower parts of the catchment (Pánek et al., 2011). The lowermost parts of the catchment are formed by thin-bedded claystone of the Lhotka Formation (Menčík et al., 1983). This material is highly susceptible to denudation with regional minimum mean mechanical denudation rates varying between 2.5 and 13.4 mm ky^{-1} (Danišík et al., 2008; Baroň et al., 2010; Pánek et al., 2010). The region and the catchment itself bear a high number of landslides and other slope deformations (e.g. Záruba, 1922; Krejčí et al., 2002; Smolková, 2011;Pánek et al., 2013a; Pánek et al., 2013b; Lenart et al., 2014).

The hydrological regime of the river is controlled by melting snow and spring/summer rainfall. The present climate in the region is mountainous and the region is one of the coldest, rainiest and windiest in the Czech Republic - the average annual rainfall and temperature on the Lysá Hora summit is 1391 mm and 2.6°C, respectively (Tolasz, 2007). The study area (ca. 4 km^2) is situated in the upper part of Satina river catchment at an elevation between 500 and 1000 m a.s.l. The valley is V-shaped, narrow and deep in the upper stretch and wider and fringed by the colluvial accumulations on one or both sides in the middle stretch. In the lowermost stretch, the valley is U-shaped with ~15 m deep rocky canyon formed on its bottom. All the side valleys in the study area are hanging.

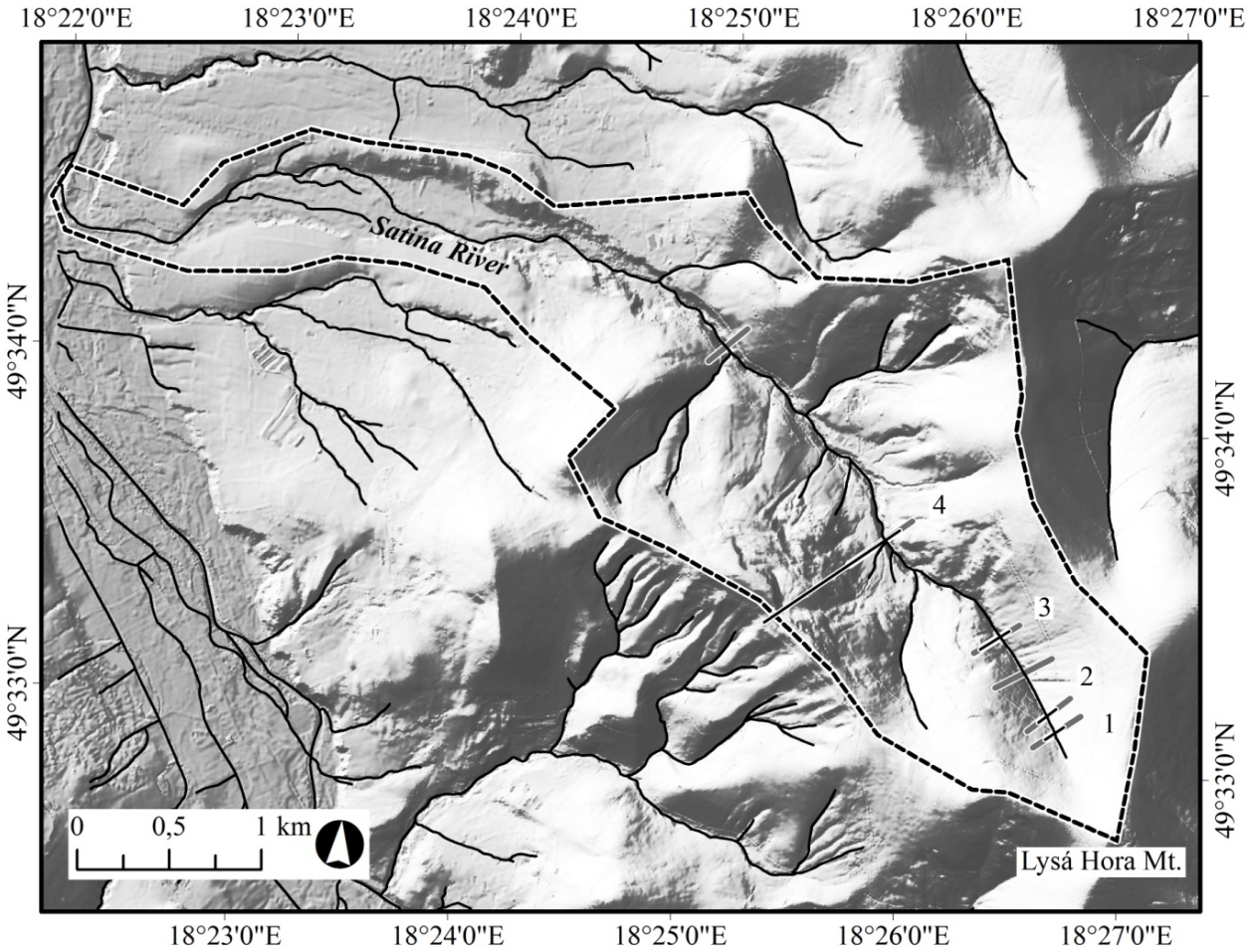

Figure 1. Map of studied catchment (dashed line) with marked discussed geophysical transects (numbered black lines) and topographical profiles (grey lines)

Pánek et al., (2011) described a deep seated disintegration of the Lukšinec ridge (NW trending spur of the Lysá hora Mountain that delimits left side of the Satina river catchment) and Šilhán (2012b) identified in one of the Satina River high-gradient right-side hanging tributaries 26 out of last 113 years as years of rapid geomorphological processes, namely flash floods and debris flows. Tichavský et al., (2014) reckoned meteorological conditions (extreme daily precipitation and rapid snowmelt) as a major trigger of activation of debris flows in the high-gradient streams on the southern slope of Lysá hora Mountain during last 75 years.

The Satina river valley was not directly affected by the Pleistocene glaciations, as the mountain glaciers were not formed in this part of Carpathians and the continental glacier stopped just in the foreland of the Western Beskids during its maximum extent in Saalian 1 (Ehlers & Gibbard, 2004; Nývlt et al., 2011). Contrary to the uppermost part of the studied area, where the climax sparse deciduous trees predominate on the blockfields and steep slopes, in the lower parts planted dense coniferous trees dominate. The first colonization of this part of Western Beskids took place in the 16-17th centuries during so-called Wallachian colonization (Štika, 2007).

3. MATERIALS AND METHODS

To perform detailed geomorphic mapping of the highest parts of the Satina River catchment, we conducted GNSS-based geomorphic mapping with the aim of defining the extent of colluvial accumulations and exposures suitable for further detailed analyses. The precise longitudinal profile of the stream was measured using the laser range-finder with built-in inclinometer. The position and height of natural steps was measured and the steps were classified into one of two classes: steps formed i) by the bedrock and boulder accumulations and ii) by the large woody debris. The stream gradient index (SL-index) that highlights the anomalous changes in river gradients (Troiani et al., 2014) and expresses

the energy of the valley bottom (Troiani & Della Setta, 2008) was counted for stream segments with homogenous gradient (Hack, 1973).

The reconstruction of thickness and extent of colluvial deposits and valley infill was performed using electrical resistivity tomography (ERT) (Sass 2006; Beauvais et al., 2007). We applied an Automatic Resistivity System ARES (GF Instruments®) to gather 4 profiles perpendicular to the valley axis with a total length of approximately 1000 m. Considering the contrasting conductivity of the flysch bedrock, the colluvial and fluvial deposits with different porosity and grain size characteristics, the ERT method is reliable for determining their extent (Škarpich et al., 2011; Stacke et al., 2014). The Wenner-Schlumberger electrode array with 3-5 m electrode spacing and a more than 20 m depth of investigation was used (Loke, 2012). For details of each profile see table 1.

Table 1. Technical parameters of ERT measurements. The depth range is dependent on the electrode array. Abbreviations used for electrode arrays: Wa - Wenner alpha, WS - Wenner-Schlumberger, DD - Dipole-Dipole. Profile 5 is merged from two profiles (555 m + 515 m) with 110 m overlap.

Profile	Length [m]	Depth range [m]	Electrode spacing [m]	Electrode array	Number of electrodes used
1	124	20-25	4	Wa, WS, DD	32
2	124	20-25	4	Wa, WS, DD	32
3	188	38	4	WS	48
4	195	33-39	5	Wa, WS	40
5	960	<110	5	WS	192

The thickness of valley infill remnants and its sedimentary facies were observed directly in the ~19 m high natural bank outcrop in the site C (transect 4 on the Fig. 1). Detailed sedimentological analysis (the grain-size; clast shape, size, roundness and depositional analyses) was used to determine the origin of each sedimentary facie. To provide information on depositional characteristics, the *in situ* measurements of dip and azimuth of the longest axis of 50 clasts from each facie was performed using geological compass. Results were visualized in the Stereonett v 2.46 software. Every sample of 50 clasts was subsequently divided into six groups depending on its roundness and edge reworking: VA (very angular); A (angular); SA (sub-angular); SR (sub-rounded); R (rounded); WR (well-rounded) (Krumbein, 1941). The three main perpendicular axes of each of 50 clasts were measured to evaluate its shape. The MS Excel macro created by Graham & Midgeley (2000) was used to construct Triangular diagram petting spreadsheet TRI-PLOT representing clast shape continuum (Sneed & Folk, 1958). The RA/C_{40} index (Graham & Midgley, 2000) was counted from values obtained from shape and roundness analyses. The particle size distribution was established using wet sieving on the device Fritsch – system3apro (sieves with 20, 63, 200, 630, 2000, 5000 and 10000μm mesh) and the Autosieb software. 350 g bulk from each facie was divided into three size fractions: mud, sand and gravel (Krumbein & Sloss, 1963) and the results were visualized using the Gradistat software (Blott and Pye, 2001). The total organic content in the samples was determined by the loss of weight of a sample on ignition at 550°C using the methodology of Heiri et al., (2001). The facies described in the outcrop on site C were classified using methodology proposed by Miall (2006). Due to the lack of suitable material and unsuitable grain size and geological composition, no dating methods (radiocarbon, ^{7}Be, OSL) could be have been used.

The antecedent precipitation index for 30 preceding days (API_{30}) (e.g. Rose, 1998; Ali et al., 2010) for the meteorological station on the Lysá hora Mountain summit was counted for two heavy rain episodes to evaluate the effect of antecedent rainfall upon runoff in the Satina River catchment. The API_{30} for the heavy rain episodes were than compared with the average API_{30} counted for the period of years 1961-1990.

4. RESULTS

The detailed survey was conducted at three sites that are situated in the upper part of the Satina river catchment. The site A is located in the amphitheatre-shaped valley head, near the spring of the Satina River at an elevation between 900 and 1000 m a.s.l. (transects 1 and 2 on the Fig. 1). Site B (transect 3 on the Fig. 1) is located ~500 m downstream on both sides of the valley at an elevation between 700 and 800 m a.s.l. Site C (transect 4 on the Fig. 1) is located on the left side of the valley ~800 m downstream from the site B at an elevation between 650 and 850 m a.s.l.

4.1. Landscape characteristics documented by geomorphic mapping and analysis of longitudinal and transversal profiles

A geomorphological survey reveals a ca. 7 km long and up to 1.5 km wide valley on the NW slope

of the Lysá hora mountain with multiple slope deformations (landslides, debris flows), and erosional landforms (gullies) on both sides of the valley. The largest slope deformation (site C) (Fig. 2) covers the slope in the area of nearly 1.5 sq. km from the Lukšinec ridge downhill to the valley fringe where the ~20 m high terrace is preserved. The smaller, yet more distinctive landslide with preserved significant accumulation that deflected the Satina River stream was found at the site B. The present-day valley bottom is in the uppermost reach filled with boulder accumulations of variable thickness. The valley bottom is filled by thin accumulation of gravel deposits in the wider lower reaches. These deposits are presumably formed by gravel bars and lobate accumulations of debris flows. The narrow river channel is vertically cut into the bedrock in few shorter segments (e.g. site C) and in some reaches disappears in the boulder accumulations (site B).

According to the longitudinal profile and the SL-index (Fig. 3), the Satina River exhibits in its upper course features of a high-energy stream. The river on its course crosses numerous steps formed by the emerging resistant thick sandstone beds and boulder or large woody debris (LWD) accumulations. The figure 3 clearly shows the higher stream energy in the reaches, where step or sequence of steps is present. The SL-index also demonstrates changes in the reaches where stream crosses the contact of the geological units. The Satina river crosses in the study area 92 steps higher than 0.5m. Fifty-eight steps are formed by the boulder accumulations, five are formed by the LWD and 29 are formed by the emerging bedrock. The mean height of the boulder, LWD and bedrock step is 1 m, 1.6 m and 1.3 m, respectively. The absolutely highest step (height of 3.5 m) is located 1190 m downstream from the spring and is formed by the emerging sandstone bed (the so-called Satina River waterfall). From the 430 m of total vertical difference between Satina river spring and the lower end of the study area, the river descends 102m over the steps (56m over boulder steps, 38m over bedrock steps and 8 m over LWD steps).

In the uppermost river reach steps formed by the boulder accumulations predominate. In a downstream direction the number of steps formed by the bedrock increase. Contrary to the similar streams in the Western Beskids (Galia & Hradecký, 2014) only five steps (height: 2.5; 2; 2; 1 and 0.5 m) formed by the LWD are present.

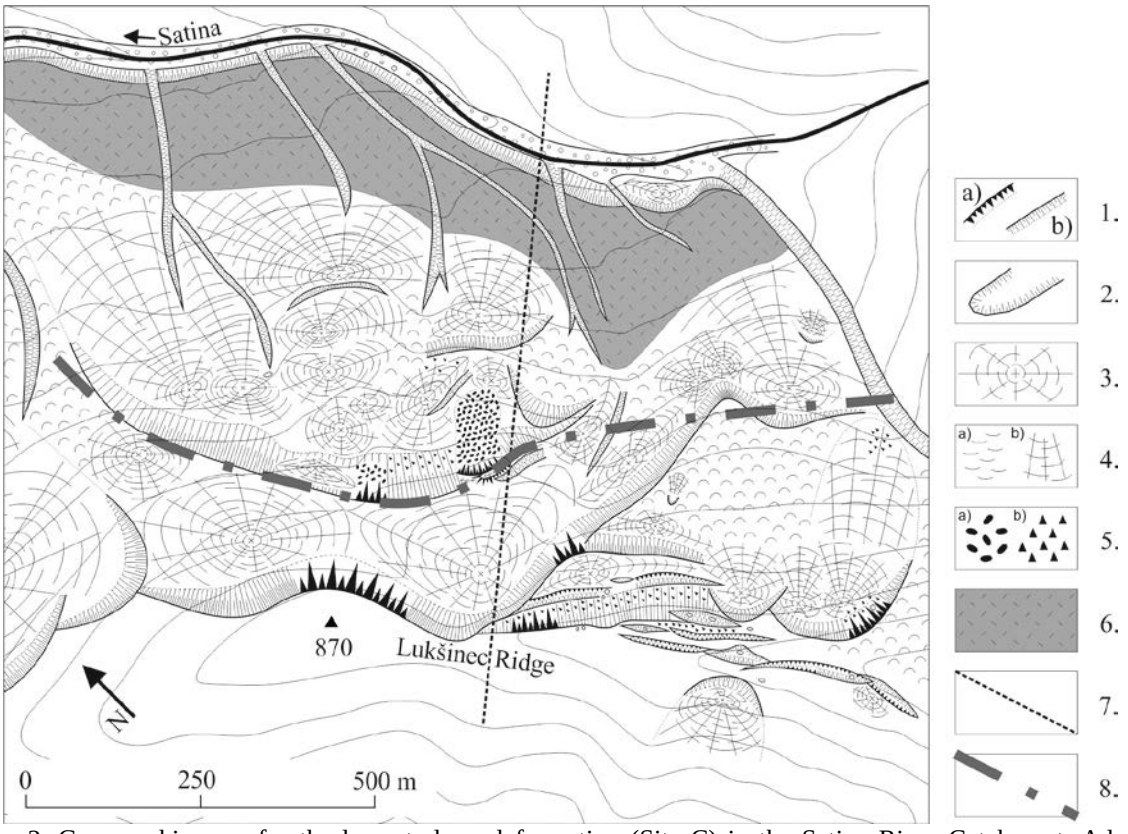

Figure 2. Geomorphic map for the largest slope deformation (Site C) in the Satina River Catchment. Adapted from Pánek et al., 2011. (1 – headscarp (a – rocky, b – soil mantled); 2 – trench, sinkhole-type depression; 3 – colluvial swell (landslide block); 4 – landslide body (a – creeping slope, b – colluvial tongue); 5 – talus (a – large blocks, b – debris slope); 6 – colluvial accumulations; 7 – ERT profiles 4+5; 8 – lithological boundary between thick- (upper part of the slope) and thin-bedded flysch formation (lower part of the slope))

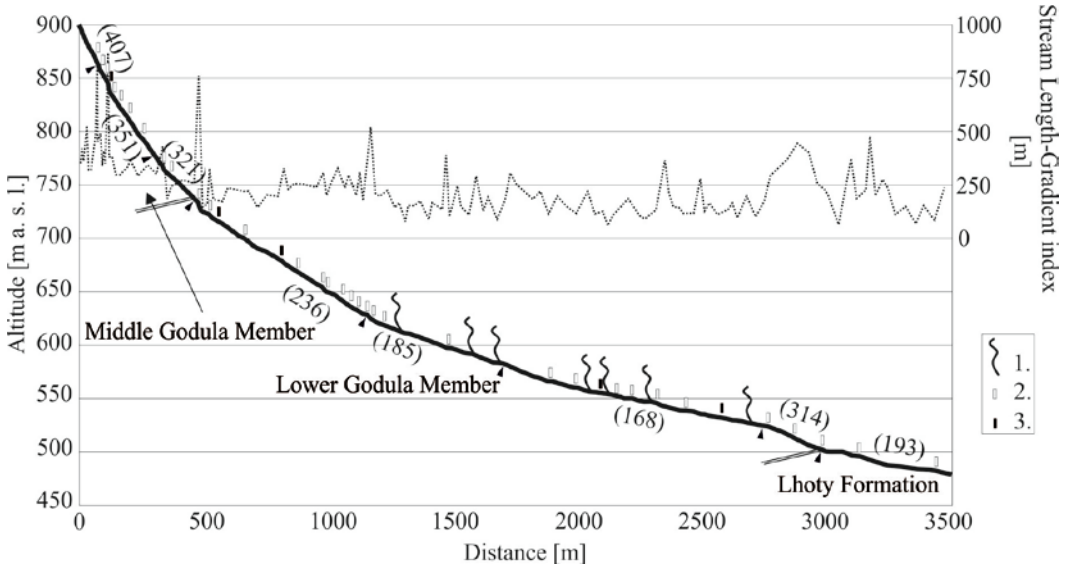

Figure 3. Longitudinal profile with SL-index of the Satina River with marked main geological units. Numbers in brackets indicate the SL index of the River stretches between triangle marks. (1 – hanging tributaries; 2 – steps formed by the rock accumulations or emerging bedrock, higher than 1 m; 3 – steps formed by LWD)

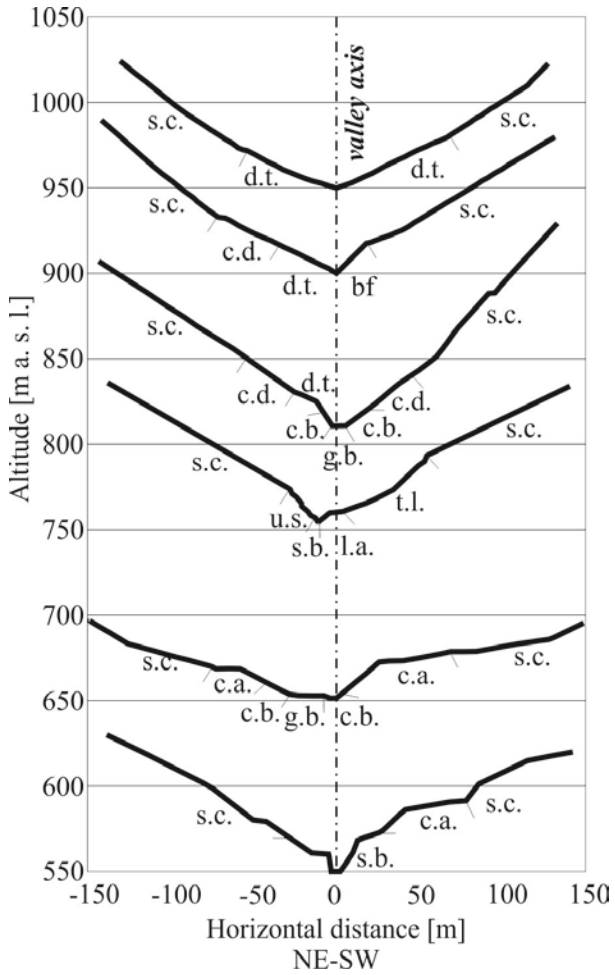

Figure 4. Transversal profiles across the Satina River valley bottom. (bf – blockfield; c.a. – colluvial accumulation; c.b. – thinly laminated claystone bedrock; c.d. – colluvial debris; d.t. - debris talus; g.b. – gravel bar; l.a. - landslide accumulation; s.b. – sandstone bedrock; s.c. – soil covered colluvium; t.l. - translational landslide; u.s. - undercut slope)

Based on the comparison of the transversal profiles across the valley (Fig. 4), river was segmented into the four reaches distinguished according to the differences in the slope and valley bottom morphology. The first reach in the amphitheatre-shaped valley head is represented by the V-shaped valley. Downstream, the widening of the valley is prominent and the slopes are undercut or covered by the colluvial debris (second reach). Third reach is characteristic by the thick accumulation preserved under the slopes on one or both sides of the valley. Fourth reach is situated in the lowermost part of the study area and the gorge with vertical walls is well preserved here.

4.2 Geophysical dataset

Within the geophysical survey of the Satina river infill and adjacent slopes, five ERT profiles were performed in order to determine i) extent and depth range (thickness) of valley fill deposits; ii) extent and depth of slope deformations; iii) connections between slope and fluvial forms within slope channel system/coupling.

For the ERT survey of the valley infill, and also due to difficult electrode grounding conditions (block fields, debris), the Wenner alpha electrode configuration was used (for its good resolution of horizontal structures and lower sensitivity to transitional resistance). For deeper investigation of the slope deformation, the Wenner-Schlumberger electrode array was chosen (Karous, 1989; Zhou et al., 2002; Milsom, 2005; Kneisel, 2006; Schrott & Sass, 2008). Details of the ERT measurements are summarized in table 1.

Two ERT measurements (Profile 1 and 2; Fig. 5) were performed in the Site A across the blocky- and debris infill where the river stream runs under the surface through boulder accumulations. Three the most often used electrode configurations (Zhou et al., 2002; Milsom, 2005; Loke, 2012) – Wenner alpha (Wa), Wenner-Schlumberger (WS) and dipole-dipole (DD) arrays were tested in order to determine range/extent and depth/thickness of the blocky and debris colluvial deposits. All of the arrays and resistivity models respectively, clearly depict range/extent and depth/thickness of the blocky and debris colluvial deposits. Thickness reaches up to ~ 7 m, and it is represented by modelled resistivity values >2000Ω.m within Profile 1. Sandstone-dominated flysch bedrock series are represented by values ranging from first hundreds of Ω.m to 2000 Ω.m, while higher values ca. 1000-2000 Ω.m indicate the presence of more rigid sandstone blocks. Very similar situation is depicted on Profile 2 which was situated ca 200 metres downstream, where amphitheatrical valley head gradually change into a gorge.

Profile 3 (Fig. 5) was conducted another ~500m downstream in the V-shape reach of the Satina River (Site B). The aim of this profile was to capture a situation of the shallow translational landslide from 1997. The 1997-landslide originated on the contact of sandstone-dominated flysch bedrock (***sfb***) (>100 Ω.m) and claystone-dominated flysch complex (***cfb***) (<100 Ω.m), what is clearly displayed in the ERT model of the Profile 3. Resitivity values ca. 1000-2000 Ω.m probably stand for rigid sandstone blocks and values higher than 2000 Ω.m represent block fields (thickness ca 10m), that evolved on the more moderate parts of the slopes.

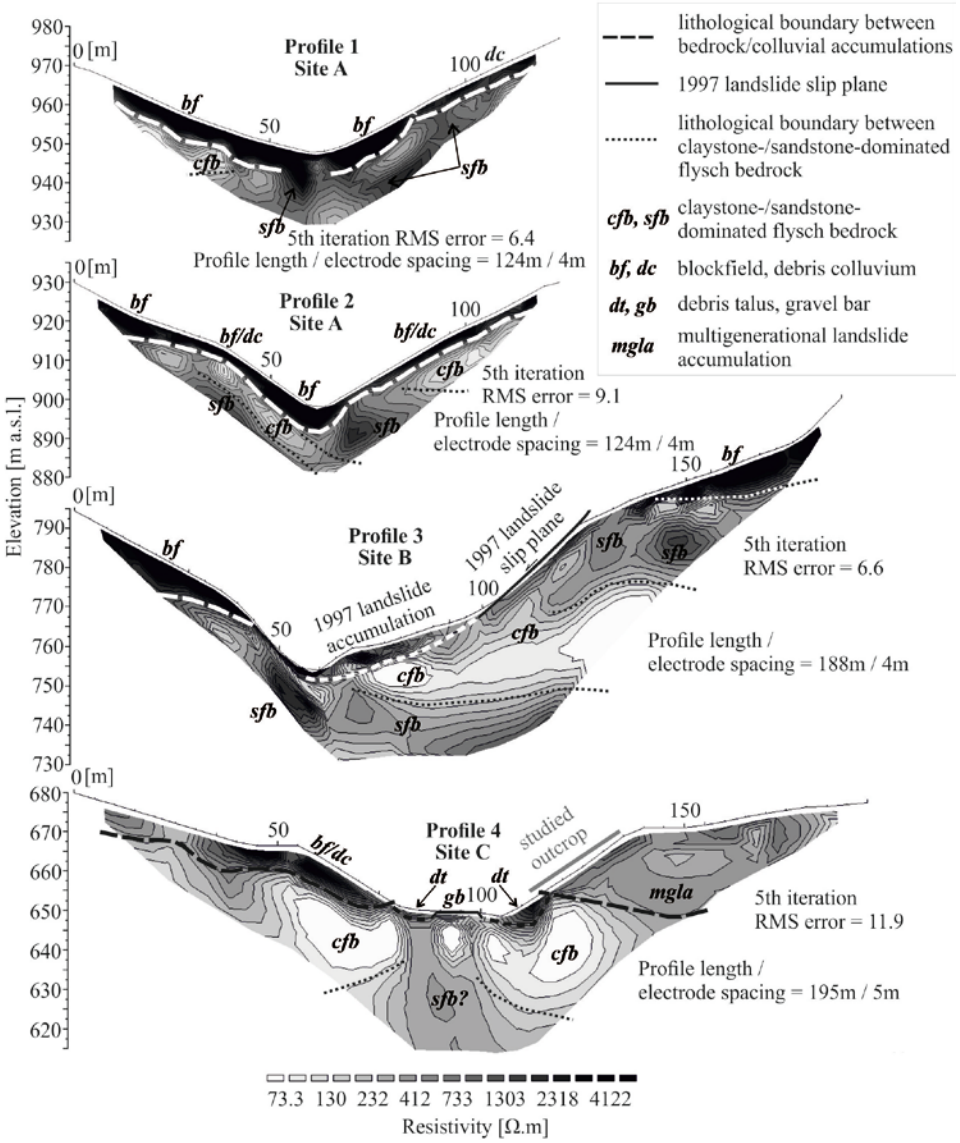

Figure 5: Electrical resistivity tomography transects across the studied valley. For the location of transects, see figure 1.

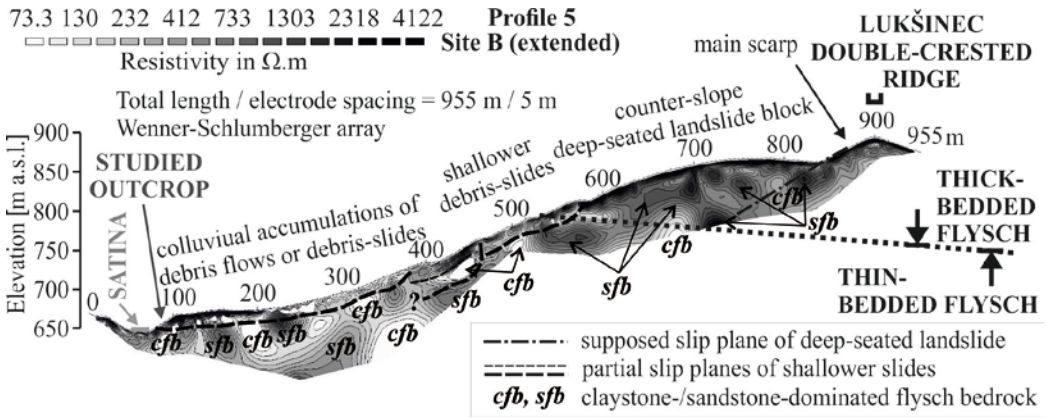

Figure 6. Electrical resistivity tomography transect from the Lukšinec Ridge to the Satina Valley bottom

Profile 4 (Fig. 5) captures the situation of the Site C, where river incised into 19 m thick multigenerational flowslide and debris flow accumulation and another 4 metres into the thin-bedded claystone-dominated bedrock. As regards the particular resitivity values, we can recognize claystone-rich series (<100 Ω.m), sandstone bed (100-900 Ω.m), and block field/debrisfield (>1000 Ω.m). Very interesting part of the profile (105-195 m on Profile 4) displays a multigenerational sedimentary set comprised mainly of accumulation of the debris flow, flowslides or debris taluses (***mgla***). Resistivity of these sedimentary series is ranging between ca. 500-2000 Ω.m. Above-mentioned accumulation (***mgla***) was investigated in detail within natural outcrop (see chapter 4.3 and Fig. 7).

Profile 5 (Fig. 6) with total length 960m consists from two inline profiles with 110m long overlap. This merged profile gives us the evidence of the extensive disintegration of the slope adjacent to the Satina valley. Profile was carried out in prolongation of the Profile 4 up to the Lukšinec Ridge. Thus it covers the whole slope (thought as in profile line) from Satina river bed (650 m a.s.l.) to the Lukšinec Ridge (900 m a.s.l.). Total vertical exaggeration (elevation difference) of the profile is 250 m.

Similarly to the profiles mentioned above, different resistivity values can be defined as changing lithological and structural condition of the subsurface. As regards small values of resistivity (<100 Ω.m), we can recognize prevailing claystone rock or clay-rich colluvium. Higher values, ranging from 100 to 1000 Ω.m, can be assigned to the sandstone formation or sandstone colluvium with separate rigid block with higher resistivity (thousands Ω.m). Also block fields have such high resistivity pattern.

4.3 Facies composition and distribution

The facies forming the ~19 m thick remnants of former valley infill were described in the natural outcrop in the left bank of the Satina river (site C) (Figs. 7 and 8). Fifteen layers of different origin were identified and according to Miall (2006) classified into 6 lithofacies from the partial sedimentological features. The surface layer ca. 40 cm thick is formed by the sandy cambisol (Němeček, 2001) with sporadic clasts and rhizosphere covered by 10 cm thick layer of the sandy forest litter.

The **Gmm** facie (sensu Miall, 2006) is formed by large sandstone boulders and blocks supported by the dry, loose matrix with the greyish brown colour. In the matrix the heterometric gravel, sand and coarse silt predominate. The 52 % of the outcrop height was formed by this facies. The largest boulders and blocks (length of the longest axis up to 1 m) were described in the basal part of every single layer and in the upward direction size of boulders significantly decreased (length of the longest axis up to 40 cm). The thickness of each Gmm facie is between 0.65 m and 1.6 m. On the planar sub-horizontal bounding surfaces the amalgamation was developed and the resulted thickness of the series of overlying Gmm facie was up to 4 m. The horizontal thin clayey ochre-coloured intercalations were developed in the places, where ground water formed small springs.

The blocks and boulders (length of the longest axis up to 0.5 m), smaller partially rounded cobbles, angular clasts and claystone fragments largely prevail in the **Gmg** facie (sensu Miall, 2006). The gray to brown matrix consists of the middle gravel and very coarse sand; the small amount of fine sand to fine silt can also be traced in this facie. The bounding surfaces of this facie are well-marked, planar and sub-horizontal. The colour is more gray or brown in the layers with higher amount of clay or sand, respectively. The overall thickness of Gmg facie is 3.15 m and forms 28% of total outcrop height.

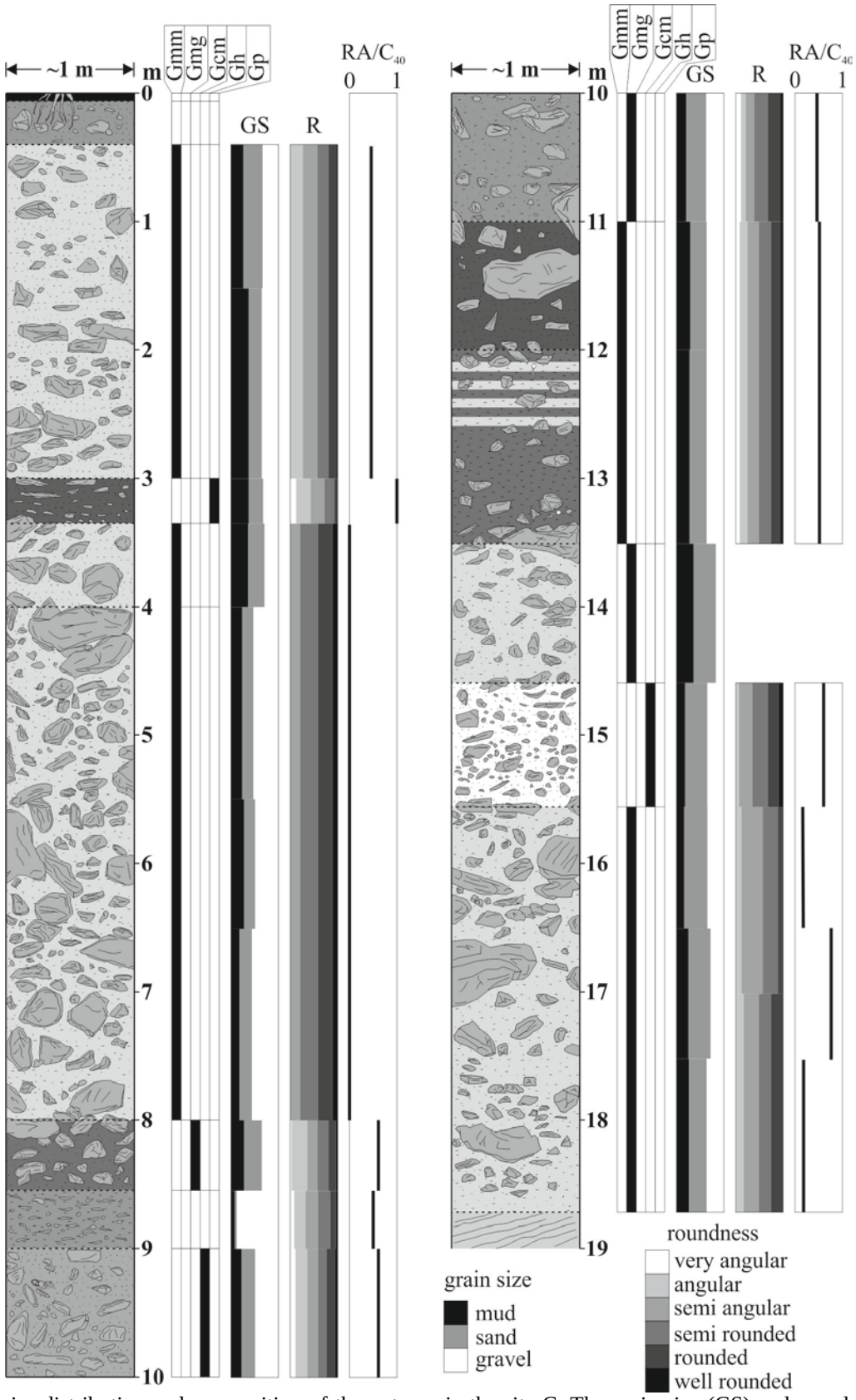

Figure 7. Facies distribution and composition of the outcrop in the site C. The grain size (GS) and roundness (R) are expressed as a percentage of the analysed fraction and roundness category, respectively.

The **Gcm** facie (sensu Miall, 2006) is composed by the cobbles (length of the longest axis up to 20 cm). The middle gravel and sand forms the pale gray to brown matrix. This facie is present in the single 0.55 m thick layer and forms 3% of total outcrop height. Both upper and lower bounding surfaces are sub-horizontal and well-marked.

The small partly rounded clasts (length of the

longest axis 5-10 cm) prevail in the **Gh** facie (sensu Miall, 2006). The dry, gray matrix is composed of fine to very fine gravel with some sand and very coarse silt. This facie forms 10.5 % of total outcrop height in two layers of thickness 1 m and 0.95 m, respectively.

The **Gp** facies (sensu Miall, 2006) is formed by small clasts that exhibit imbrication especially in the lower part of the layer. The middle gravel and fine silt prevail in greyish matrix. The only single 0.4 m thick layer forms 2% of total outcrop height. Bounding surfaces of this layer are sub-horizontal and well marked.

The facie **H** could not be classified according to classification proposed by Miall (2006). This facie is present in single 0.45 m thick distinctive layer and forms 2.5 % of total outcrop height. This facie is solely composed of angular middle gravel-sized claystone clasts and bounded by well-marked sub-horizontal bounding surfaces. The rare matrix is ochre coloured, clayey and plastic. The analysis of clast orientation was impossible due to its small size.

According to classification proposed by Miall (2006), facies Gmm and Gmg could be interpreted as accumulations of multigenerational accumulations of debris flows.

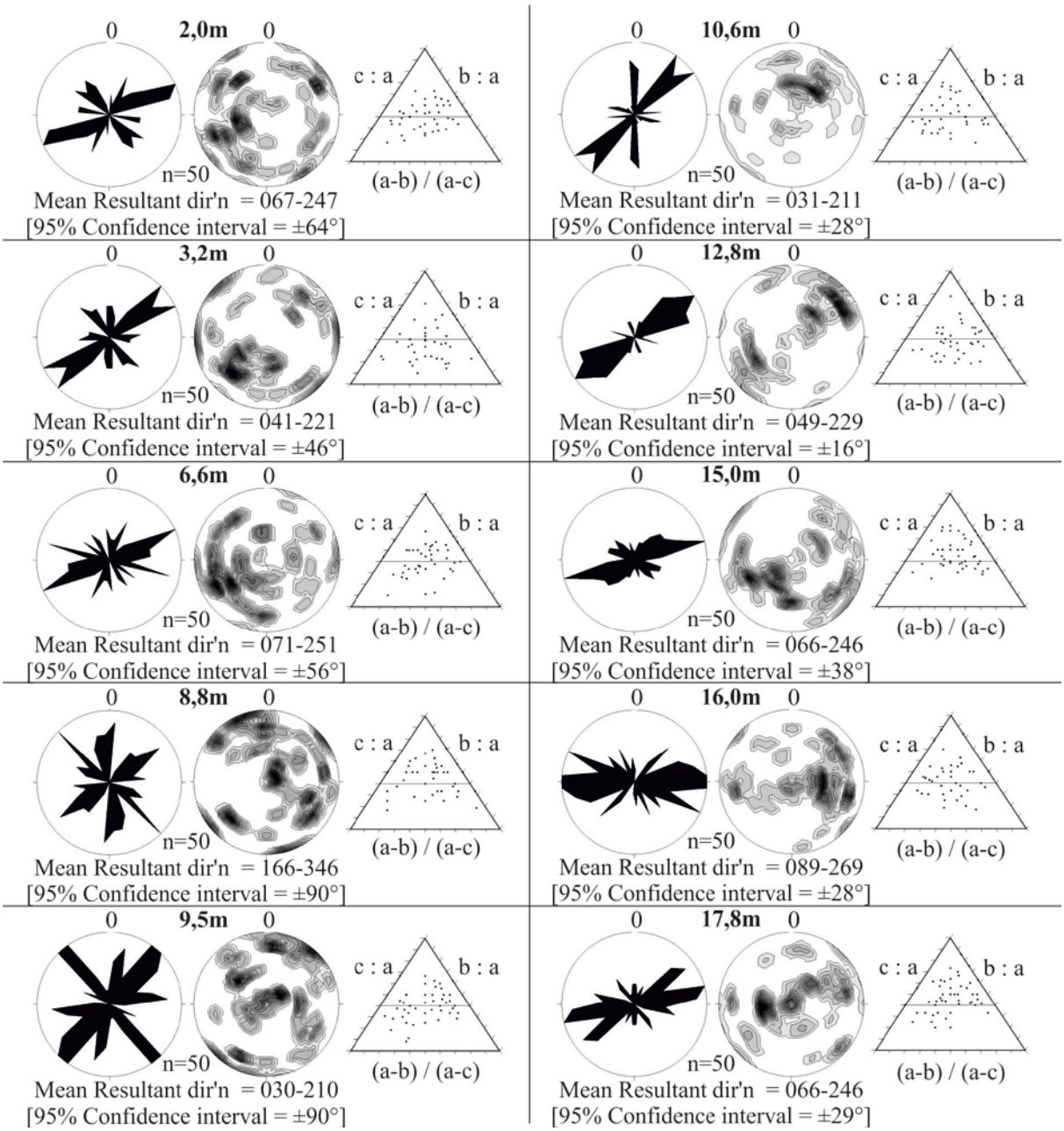

Figure 8. Azimuth and dip of the longest axis of clasts and clast shape continuum of the selected facies in the outcrop in the site C.

Facies Gh could be interpreted as accumulations of debris flows, that were from upper parts of the catchment transported and re-deposited in fluvial environment of the Satina river. Facies Gcm could be interpreted as deposits of proluvial fan. Facies H could not be according to classification proposed by Miall (2006) properly classified, but could be interpreted as thicker claystone bed, transported by slope processes and *in situ* weathered to its present form. Genetic classification of facies Gp is very problematic, but according to our observations the fluvial or periglacial origin and transport are most probable.

5. DISCUSSION

The Satina River continuously alters the shape and gradient of its valley bottom and adjacent slopes. The headward erosion is gradually reshaping the U-shaped valley into the V-shaped valley. The excellent example of this transition can be found in the site A. Contrary to the section above the spring where the valley is U-shaped, the initial stage of transition into the V-shaped can be observed only few tens of meters under the spring (compare profile 1 and 2 on the Fig. 4).

The SL-index (Fig. 3) exhibits the increased energy of the Satina River on the contact of two geological units. Šilhán (2012b) described the area on the contact zone of two geological units as an evident source zone of debris flow material in one of the right high-gradient tributaries of the Satina River. Thus, the geological structure of the Lysá hora Mt. influences processes on the slopes and in the stream as well.

The entire slope of the Lukšinec ridge (part of the Lysá hora Mountain group adjacent to the Satina River) is affected by the deep disintegration and is an excellent example of the deep-seated gravitational slope deformation (DSGSD). Morphological evidence of deep-seated slope failure can be found namely in the double-crested ridge area – tension cracks and counter-slope scarps up to ~3 meters deep, numerous rock outcrops with block disintegration, sinkhole-type depressions – all as a result of the various types of slope movements such as sackung, lateral spreading, toppling or incipient sliding (Hradecký & Pánek, 2008; Pánek et al., 2009; Pánek et al., 2011). Lenart et al., (2014) described connection of fissure cave systems (Ondrášovy díry and Ledová jeskyně caves) located in the uppermost part of the Lukšinec ridge with the development of these slope failures.

The upper sections of the slopes adjacent to the Satina Valley are thus loosened by the block movements (sackung, lateral spreading) and other processes mentioned above. A massive rockslide with typical toppling of massive sandstone blocks and consequent rock falling and developed blockfield at the toe of the freeface evolved on the left slope of the Satina River valley above site C (Pánek et al., 2011).

Contiguous (middle and lower) parts of the slopes are affected by shallower slope processes such as flow-type debris slides and debris flows. Their occurrence is closely related to the loosened slope and accumulations of the deeper landslides higher on the slope. These accumulations form the source area for the consequent shallower deformations. Some of the flowslides and debris flows have a relatively long run-out and their colluvial lobes often reach the valley bottom. We can distinguish two types of slope-channel interactions – i) a partial damming of the valley by shallow landslide accumulation with a deviation of the river course (site B); ii) complete damming of the valley bottom with subsequent river incision (site C). This slope-channel coupling represents a sediment transport system which includes transfer of sediments from the ridge parts of the Lukšinec down to the Satina River valley bottom. We can observe a concatenation of the slope and fluvial processes. The higher situated accumulations act as a source areas for the subsequent processes within the spatio-temporal system: deep-seated ridge disintegration – deep seated rockslides and landslides – shallower flow slides and debris flows – colluvial lobes and proluvial cones – alluvial accumulations (gravel bars, terraces).

Essential for understanding of the deep-seated disintegration of the Lukšinec ridge is the lithological boundary in upper third of the profile (Fig. 2 and 5). The boundary divides bedrock into two formations (Middle- and Lower Godula Member of the Outer (Menilite-Krosno) Group of Nappes), which consists of the thick-bedded flysch rock with prevailing sandstones (***sfb***) and the thin-bedded (claystone-dominated) flysh formation (***cfb***), respectively. Underlying claystone or mudstone acts as a slip surface (sheer surface) for the slow deep-seated ridge disintegration. The processes of lateral sprading and sagging prevail in the upper parts of the profile (and slope). On one specific site also toppling and consequent rockfalling occurs. The upper third of the profile can be characterized as a large block deep-seated landslide with very well pronounced main scarp (ca 40 m of vertical height). The landslide block is intensively disrupted. According to the assumed position of the slip plane we can estimate the landslide thickness to ~50 m. Middle and lower parts of the landslide can rather be

characterized as affected by shallower (still up to tens of metres) slope deformations, such as landslides, flowslides and debris flows. These conlusions are also supported by the results of resistivity tomography (ERT) which show structure and thickness of colluvial (landslide) bodies. ERT also indicates, by means of resistivity values, the above mentioned bedrock boundary between ***sfb*** and ***cfb***. The distal colluvial lobe dammed (partly at least) the valley in the past. River incision then caused 22 m height natural outcrop, which was studied by sedimentological analyses (see chapter 4.3).

The remnants of the Satina River valley sedimentary infill (site C) are according to our results formed by multiple generations of debris flow accumulations or the landslide accumulation fronts. These processes are in the lesser extent still active in the upper parts of the catchment (site B), where the shallow translational landslide was activated after two heavy rain episodes in the summer 1997. During first episode (from July 5th to July 8th) the total precipitation reached 571 mm and the Antecedent Precipitation Index (API_{30}) was 138.8 mm (187% of the average); during the second episode (from July 18th to July 20th) the total precipitation reached 146.8 mm and the API_{30} was 321.9 mm (389% of the average). The saturated subsurface (max. depth ~3 m) part of the slope slipped and partly dammed the valley. Current stream was deflected by the landslide accumulation (which is also well recognizable) and now is affecting both adjacent slope and the accumulation itself. This combination of lateral erosion and vertical incision may cause future destabilisation of the slopes or reactivation of temporarily inactive landslide accumulation (thickness max ca. 8 m). The water ran through the accumulation with no evidence of the water within current river channel in the course of the ERT measurement (November 2013). Also, the deposits of the 1997-landslide would serve as a sediment source of the Satina river within slope-channel coupling. The fluvial intercalations in the sedimentary infill (facies Gh and Gp, site C) were deposited most probably during the relatively short events when the valley was completely dammed by the debris flow accumulations.

The Satina River banks were eroded and the sandstone boulder settled on the edge of the valley (volume ~113 m^3; estimated weight ca. 250 tons) rolled down to the stream during the two heavy rain episodes in the spring 2010. The Satina River vertically cut ~1.5 m into the thinly laminated claystone bedrock in the site C during these episodes. The total precipitation reached 362.7 mm and the API_{30} was 99.2 mm (207% of the average) during the first episode (from May 15th to May 20th); total precipitation reached 131.6 mm and API_{30} was 223 mm (366% of the average) during second episode (from May 30th to June 3rd).

6. CONCLUSION

The Satina River continuously alters the shape and gradient of its valley bottom and adjacent slopes. The headward erosion is changing the valley shape from the U-shaped to the V-shaped in the upper parts of the Satina River catchment where the valley is fringed by the colluvial accumulations. The vertical erosion formed the canyon-like shaped valley in the lower parts of the study area where the river is vertically cut ca. 18 m into the multigenerational deposits of debris flows with fluvial intercalations and another ~3 m into the bedrock.

The slopes of the Lysá hora Mountain group are widely affected by the slope deformations of almost all types. These processes include the slow deep-seated creep accompanied by lateral spreading, toppling, sagging and rock sliding, shallow debris slides and debris flows (sensu Dikau et al., 1996) and are the sources of sediment budget in the Satina river catchment.

The shallow landslide was reactivated and partly dammed the valley after the heavy rain episode in the summer 1997. Stream was deflected by landslide accumulation and now is undercutting the adjacent slope. This destabilization of the slope may lead to the activation of landslide on the opposite side of the valley and ultimately to the complete damming of the valley. Alteration of similar processes most probably led to deposition of massive accumulation in the lower parts of the catchment.

The studied part of the catchment is thus characterized by the geomorphological processes pattern change observed in the formation of a large accumulations most probably in the transport limited conditions of a colder period of the Pleistocene (forest-free area) and prominent intensive vertical cutting in the supply limited conditions of the Holocene. This example of interaction of slope and fluvial processes illustrates the Holocene evolution of the Satina River valley and most probably the adjacent valleys as well.

Acknowledgement

This work was supported by the project NEXLIZ CZ.1.07/2.3.00/30.0038, which is co-financed by the

European Social Fund and the state budget of the Czech Republic and the GAUK project no. 862213 which is financed by the Grant Agency of Charles University in Prague. The authors are grateful to Tomáš Pánek and Karel Šilhán for valuable comments and advices during the field work.

REFERENCES:

Alexandrowicz, S.W., 1993. *Late Quaternary landslides at eastern periphery of the National Park of the Pieniny Mountains, Carpathians, Poland.* Studia Geologica Polonica 192, 209–225.

Alexandrowicz, S.W. & Alexandrowicz, Z., 1999. *Recurrent Holocene landslides: a case study of the Krynica landslide in the Polish Carpathians.* The Holocene, 9, 91–99.

Ali, S., Ghosh, N.C. & Singh, R., 2010. *Rainfall-runoff simulation using a normalized antecedent precipitation index,* Hydrological Sciences Journal, 55, 2, 266-274.

Bábek, O., Faměra, M., Hilscherová, K., Kalvoda, J., Dobrovolný, P., Sedláček, J., Machát, J. & Holoubek, J., 2011. *Geochemical traces of flood layers in the fluvial sedimentary archive; implications for contamination history analyses.* Catena, 87, 281-290.

Baroň, I., 2007. *Results of radiocarbon dating of deep-seated landslides in the area of Vsetín and Frýdek-Místek districts*. Geologické výzkumy na Moravě a ve Slezsku, 14, 10–12.

Baroň, I., Baldík, V. & Fiferová, M., 2010. *Preliminary assessment of a recent denudation rate of the Flysch Belt of Outer West Carpathians – Case study: Bystřička River catchments in Vsetínské Hills.* Geologické výzkumy na Moravě a ve Slezsku, 17, 10-13.

Baroň, I., Bíl, M., Bábek, O., Smolková, V., Pánek, T. & Macur L., 2014. *Effect of slope failures on river-network pattern: A river piracy case study from the belt of the Outer Western Carpathians.* Geomorphology, 214, 356-365.

Beauvais, A., Parisot, J.C. & Savin, C., 2007. *Ultramafic rock weathering and slope erosion processes in a SW Pacific tropical environment.* Geomorphology, 83, 1-13.

Blott, J.S. & Pye K., 2001. *Gradistat: a grain size distribution and statistics package for the analysis of uncosolidated sediments.* Earth Surface Processes and Landforms, 25, 1473–1477.

Brown, A.G., Carrey, C., Erkens, G., Fuchs, M., Hoffmann, T., Macaire, J-J., Moldenauer, K-M. & Walling, D.E., 2009. *From sedimentary records to sediment budgets: Multiple approaches to catchment sediment flux*. Geomorphology, 108, 35-47.

Coulthard, T. & Macklin, M., 2001. *How sensitive are river systems to climate and land-use changes? A model-based evaluation.* Journal of Quaternary Science, 16, 347–351.

Chiriloaei, F., Rădoane, M., Perşoiu, I. & Popa, I., 2012. *Late Holocene history of the Moldova River Valley, Romania,* Catena, 93, 64-77.

Danišík, M., Pánek, T., Matýsek, D., Dunkl, I. & Frisch, W., 2008. *Apatite fission track and (U-Th)/He dating of teschenite intrusions gives time constraints on accretionary processes and development of planation surfaces in the Outer Western Carpathians.* Zeitschrift für Geomorphologie, 52, 273–289.

Derwich, M., & Żurek, A. (Eds.), 2002. *By the Roots of Poland (up to the year 1038) (In Polish).* Wydawnictwo Dolnośląskie. Wroclaw.

Dikau, R., Brunsden, D., Schrott, D. & Ibsen, M. L., 1996. *Landslide recognition: identification, movement and causes***.** Wiley, 251 p.

Ehlers, J. & Gibbard, P. L. (Eds.), 2004. *Quaternary Glaciations - Extent and Chronology: Part I: Europe*. Elsevier.

Galia, T. & Hradecký, J., 2014. *Morphological patterns of headwater streams based in flysch bedrock: Examples from the Outer Western Carpathians.* Catena, 119, 174-183.

Gębica, P., Starkel, L., Jacyšyn, A. & Krąpiec, M., 2013. *Medieval accumulation in the Upper Dniester river valley: The role of human impact and climate change in the Carpathian Foreland.* Quaternary International, 293, 207-218.

Graham D.J. & Midgley N. G., 2000. *Graphical representation of particle shape using triangular diagrams: an Excel spreadsheet method.* Earth Surface Processes and Landforms, 25, 13, 1473-1477.

Grygar, T., Světlík, I., Lisá, L., Koptíková, L., Bajer, A., Wray, D.S., Ettler, V., Mihaljevič, M., Nováková, T., Koubová, M., Novák, J., Máčka, Z. & Smetana, M., 2010. *Geochemical tools for the stratigraphic correlation of floodplain deposits of the Morava River in Strážnické Pomoraví, Czech Republic from the last millennium*. Catena, 80, 106-121.

Hack, J.T., 1973. *Stream-profile analysis and stream-gradient index*. Journal Research U.S. Geological Survey, 1, 4, 421-429.

Harvey, A.M., 2001. *Coupling between hillslopes and channels in upland fluvial systems: Implications for landscape sensitivity, illustrated from the Howgill Fells, northwest England.* Catena, 42, 225-250.

Heiri, O., Lotter, A.F. & Lemcke G., 2001. *Loss on ignition as a method for estimating organic and carbonate content in sediments: reproducibility and comparability of results*. Journal of Paleolimnology, 25, 101-110.

Hradecký, J. & Pánek, T., 2008. *Deep-seated gravitational slope deformations and their influence on consequent mass movements (case studies from the highest part of the Czech Carpathians)*. Natural Hazards, 45, 235-253.

Hradecký, J., Pánek, T. & Břízová, E., 2004.

Contribution to the geomorphology and the age of the selected slope deformations in the area of Slezské Beskydy Mts. and Jablunkovská Brázda Furrow. Geografie, 109, 289–303.

Hradecký, J., Pánek, T. & Klimová, R., 2007. *Landslide complex in the northern part of the Silesian Beskydy Mountains (Czech Republic)*. Landslides 4, 53–62.

Huhmann, M. & Brückner, H., 2002. *Holocene terraces of the Upper Dnister. Fluvial morphodynamics as a reaction to climate change and human intrusion*. Zeitschrift für Geomorphologie N.F., Supplementband, 127, 67-80.

Huhmann, M., Kremenetski, K.V., Hiller, A. & Brückner, H., 2004. *Late Quaternary landscape evolution of the Upper Dnister valley, Western Ukraine*. Palaeogeography, Palaeoclimatology, Palaeoecology, 209, 51-71.

Kadlec, J., Grygar, T., Světlík, I., Ettler, V., Mihaljevič, M., Diehl, J.F., Beske-Diehl, S. & Svitavská-Svobodová, H., 2009. *Morava River floodplain development during the last millennium, Strážnické Pomoraví, Czech Republic*. The Holocene, 19, 3, 499–509.

Kalicki, T., 2000. *Grain size of the overbank deposits as carriers of paleogeographical information*. Quaternary International, 72, 107-114.

Kalicki, T., Starkel, L., Sala, J., Soja, R. & Zernickaya, V.P., 1996. Subboreal paleochannel system in the Vistula valley near Zabierzów Bocheński (Sandomierz Basin) (special issue). Geographical Studies (Wrocław), 9, 129–158.

Kalis, A.J., Merkt, J. & Wunderlich, J., 2003. *Environmental changes during the Holocene climatic optimum in central Europe — human impact and natural causes*. Quaternary Science Reviews, 22, 33–79.

Karous, M., 1989. *Geoelektrické metody průzkumu*. SNTL/Alfa, 424.

Keesstra, S.D., Bruijnzeel, L.A. & van Huissteden, J., 2009. *Meso-scale catchment sediment budgets: Combining field surveys and modeling in the Dragonja catchment, southwest Slovenia.* Earth Surface Processes and Landforms, 34 (11) , 1547-1561.

Kidová, A. & Lehotský, M., 2012. *Spatio-temporal variability of the morphology of braiding and laterally migrating Belá River (In Slovak).* Geographical Journal, 64, 4, 311-333.

Kneisel, C., 2006. *Assessment of subsurface lithology in mountain environments using 2D resistivity imaging.* Geomorphology, 80, 32–44.

Krejčí, O., Baroň, I., Bíl, M., Hubatka, F., Jurová, Z. & Kirchner, K., 2002. *Slope movements in the Flysch Carpathians of Eastern Czech Republic triggered by extreme rainfalls in 1997: a case study*. Physics and Chemistry of the Earth, 27, 1567–1576.

Krumbein, W.C., 1941. *Measurement and geologic significance of shape and roundness of sedimentary particles.* Journal of Sedimentary Petrology, 11, 64-72.

Krumbein, W.C. & Sloss, L.L., 1963. *Stratigraphy and Sedimentation, Second Edition.* W.H. Freeman and Company, 660.

Kukulak, J., 2003. *Impact of mediaeval agriculture on the alluvium in the San River headwaters (Polish Eastern Carpathians).* Catena, 51, 255–266.

Lenart, J., Pánek, T. & Dušek, R., 2014. *Genesis, types and succession of crevice-type caves in the Flysch Belt of the Western Carpathians.* Geomorphology, 204, 459-476.

Loke, M.H., 2012. *Tutorial: 2-D and 3-D electrical imaging surveys. User's manual.* Geotomo software, Penang.

Macaire, J.J., Bernard, J., Di-Giovanni, C., Hinschberger, F., Limondin-Lozouet, N. & Visset, L., 2006. *Quantification and regulation of organic and mineral sedimentation in a late-Holocene floodplain as a result of climatic and human impacts (Taligny marsh, Parisian Basin, France).* The Holocene, 16, 647–660.

Margielewski, W., 1997. *Dated landslides of the Jaworzyna Krynicka Range (Outer Carpathians) and their relation to climatic phases of the Holocene*. Annales Societatis Geologorum Poloniae 67, 83–92.

Margielewski, W., 1998. *Landslide phases in the Polish Outer Carpathians, and their relation to climatic changes in the Late Glacial and the Holocene*. Quaternary Studies in Poland 15, 37–53.

Margielewski, W., 2001. *Late Glacial and Holocene climatic changes registered in forms and deposits of the Klaklowo landslide (Beskid Średni Range, Outer Carpathians).* Studia Geomorphologica Carpatho-Balcanica 35, 63–79.

Margielewski, W., 2003. *Late Glacial-Holocene palaeoenvironmental changes in the Western Carpathians: case studies of landslide forms and deposits*. Folia Quaternaria 74, 1–96.

Margielewski, W., 2006. *Records of the Late Glacial–Holocene palaeoenvironmental changes in landslide forms and deposits of the Beskid Makowski and Beskid Wyspowy Mts. Area (Polish Outer Carpathians).* Folia Quaternaria 76, 1–149.

Margielewski, W. & Kovalyukh, N.N., 2003. *Neoholocene climatic changes recorded in landslide´s peat bog on Mount Ćwilin (Beskid Wyspowy Range, Outer Carpathians).* Studia Geomorphologica Carpatho-Balcanica 37, 59–76.

Margielewski, W., Krąpiec, M., Valde-Nowak, P. & Zernitskaya, V., 2010. *A Neolithic yew bow in the Polish Carpathians: Evidence of the impact of human activity on mountainous palaeoenvironment from the Kamiennik landslide peat bog*. Catena 80, 141–153.

Margielewski, W., Kołaczek, P., Michzcyński, A., Obidowicz, A. & Pazdur, A., 2011. *Record of the meso-and neoholocene palaeoenvironmental changes in the Jesionowa landslide peat bog*

(Beskid Sądecki Mts. Polish Outer Carpathians). Geochronometria 38, 138–154.

Menčík, E., Adamová, M., Dvořák, J., Dudek, A., Jetel, J., Jurková, A., Hanzlíková, E., Houša, V., Peslová, H., Rybářová, L., Šmíd, B., Šebesta, J., Tyráček, J. & Vašíček, Z., 1983. *The Geology of Moravskoslezské Beskydy Mts. and Podbeskydská pahorkatina Hillyland (In Czech).* Academia, 304.

Miall, A. D., 2006. *The Geology of Fluvial Deposits: Sedimentary Facies, Basin Analysis and Petroleum Geology.* Springer, 504.

Milsom, J., 2005. *Field Geophysics, the Geological Field Guide Series (3rd ed.).* Wiley, 232.

Němeček, J., 2001. *The Czech Taxonomic Soil Classification System (In Czech).* ČZU Praha, 78.

Nývlt, D., Engel, Z. & Tyráček, J., 2011. *Pleistocene Glaciations of Czechia*. In: Ehlers, J., Gibbard, P. L., Hughes, P.D. (eds): Quaternary Glaciations – Extent and Chronology, A closer look. Developments in Quaternary Science, 15, 37–46, Elsevier.

Opravil, E., 1974. *Moravo-Silesian Border Forest up to the Beginning of Colonization (In Czech).* Archeologický sborník, 1, 113-131.

Pánek, T., Hradecký, J. & Šilhán, K., 2009. *Geomorphic evidence of ancient catastrophic flow type landslides in the mid-mountain ridges of the Western Flysch Carpathians (Czech Republic).* International Journal of Sediment Research, 24, 88-98.

Pánek, T., Smolková, V. & Hradecký, J., 2010. *Reconstruction of a Holocene average catchment denudation from the landslide-dammed lakes in the Outer Western Carpathians*. Geophysical Research Abstracts 12, EGU General Assembly 2010, Vienna.

Pánek, T., Tábořík, P., Klimeš, J., Komárková, V., Hradecký, J. & Šťastný, M., 2011. *Deep-seated gravitational slope deformations in the highest parts of the Czech Flysch Carpathians: Evolutionary model based on kinematic analysis, electrical imaging and trenching*. Geomorphology, 129, 92-112.

Pánek, T., Smolková, V., Hradecký, J., Sedláček, J., Zernitskaya, V., Kadlec, J., Pazdur, A. & Řehánek, T., 2013a. *Late-Holocene evolution of a floodplain impounded by the Smrdutá landslide, Carpathian Mountains (Czech Republic).* The Holocene, 23, 218–229.

Pánek, T., Smolková, V., Hradecký, J., Baroň, I. & Šilhán, K., 2013b. *Holocene reactivations of catastrophic complex flow-like landslides in the Flysch Carpathians (Czech Republic/Slovakia).* Quaternary Research 80, 33-46.

Rose, S., 1998. *A statistical method for evaluating the effects of antecedent rainfall upon runoff: application to the coastal plain of Georgia*. Journal of Hydrology, 211, 168–177.

Sass, O., 2006. *Determination of the internal structure of alpine talus deposits using different geophysical methods (Lechtaler Alps, Austria).* Geomorphology, 80, 45-58.

Schrott, L. & Sass, O., 2008. *Application of field geophysics in geomorphology: advances and limitations exemplified by case studies.* Geomorphology, 93, 55–73.

Šilhán, K., 2012a. *Dendrogeomorphological analysis of the evolution of slope processes on flysch rocks (the Vsetínské vrchy Mts; Czech Republic).* Carpathian Journal of Earth and Environmental Sciences, 7, 39-49.

Šilhán, K., 2012b. *Frequency of fast geomorphological processes in high-gradient streams: Case study from the Moravskoslezské Beskydy Mts (Czech Republic) using dendrogeomorphic methods*. Geochronometria, 39, 2, 122-132.

Šilhán, K., 2014. *Chronology of processes in high-gradient channels of medium-high mountains and their influence on the properties of alluvial fans*. Geomorphology, 206, 288-298.

Šilhán, K. & Stacke, V., 2011. *The present day geomorphic activity of fluvial fan (a case study from the Moravskoslezské Beskydy Mts. based on dendrogeomorphological methods).* Moravian Geographical Reports, 19, 2, 18-29.

Šilhán, K., Brázdil, R., Pánek, T., Dobrovolný, P., Kašičková, L., Tolasz, R., Turský, O. & Václavek, M., 2011. *Evaluation of meteorological controls of reconstructed rockfall activity in the Czech Flysch Carpathians.* Earth Surface Processes and Landforms, 36, 1989-1909.

Škarpich, V., Hradecký, J. & Dušek, R., 2013. *Complex transformation of the geomorphic regime of channels in the forefield of the Moravskoslezské Beskydy Mts: case study of the Morávka River (Czech Republic)*. Catena, 111, 25-40.

Škarpich V., Hradecký J. & Tábořík P., 2011. *Structure and genesis of Quaternary infill of the Slavíč River valley (the Moravskoslezské Beskydy Mts, Czech Republic).* Moravian Geographical Reports, 19, 18-29.

Smolková, V., 2011. *Slope Deformations and their Impact on Valley Bottom Development (in the Czech Part of the Carpathians)*. (PhD thesis) University of Ostrava, Ostrava.

Smolková, V., Pánek, T. & Hradecký, J., 2008. *Fossil landslide-dammed lake in the Babínek valley (Vsetínské vrchy Hills): contribution to understanding the Holocene relief development in the flysch Carpathians.* Geologické výzkumy na Moravě a ve Slezsku v roce 2007 15, 41–43.

Sneed, E.D. & Folk, R.L., 1958. *Pebbles in the lower Colorado River, Texas—A study of particle morphogenesis*. Journal of Geology, 66, 114–150.

Stacke, V., Pánek, T. & Sedláček, J., 2014. *Late Holocene evolution of the Bečva River floodplain (Outer Western Carpathians, Czech Republic).* Geomorphology, 206, 440-451.

Starkel, L., 1995. *New data on the Late Vistulian and*

Holocene evolution of the Wisłoka River valley near Dębica. In: Starkel, L. (Ed.), Evolution of the Vistula River valley during the last 15000 years, part V. Geographical Studies, Special Issue 8(IGiPZPAN), 73–90.

Starkel, L., Soja, R. & Michczynska, D.J., 2006. *Past hydrological events reflected in Holocene history of Polish rivers.* Catena, 66, 24–33.

Starkel, L., Gębica, P. & Superson, J., 2007. *Last Glacial-Interglacial cycle in the evolution of river valleys in southern and central Poland*. Quaternary Science Reviews, 26, 2924-2936.

Škarpich, V., Hradecký, J. & Táborík, P., 2011. *Structure and genesis of the quaternary filling of the Slavíč River valley (Moravskoslezské Beskydy Mts., Czech Republic).* Moravian geographical reports, 19, 30-38.

Štika, J., 2007. *Vallachians and Vallachia: By the Genesis of Valachians, Vallachian Colonization, Origin and Genesis of Moravian Vallachia and also Carpathian Shepherd's Huts (In Czech).* Valašské museum v přírodě, Rožnov pod Radhoštěm.

Tichavský, R., Šilhán, K. & Tolasz, R., 2014. *Origin, triggers and spatio-temporal variability of debris flows in high-gradient channels (A case study from the culmination part of the Moravskoslezské Beskydy Mts.; Czech Republic).* Carpathian Journal of Earth and Environmental Sciences, 9, 3, 5-16.

Tolasz, R. (ed.), 2007. *Climate atlas of Czechia*. Czech Hydrometeorological Institute, Prague.

Tóth, E. 2001, in Köpeczi, B (ed.). *History of Transylvania: I. 3. The Roman province of Dacia*. Columbia University Press, New York.

Troiani, F. & Della Setta, M., 2008. *The use of the Stream Length–Gradient index in morphotectonic analysis of small catchments: A case study from Central Italy*. Geomorphology, 102, 1, 159-168.

Troiani, F., Galve, J. P., Piacentini, D., Della Setta, M. & Guerrero, J., 2014. *Spatial analysis of stream length-gradient (SL) index for detecting hillslope processes: A case of the Gállego River headwaters (Central Pyrenees, Spain).* Geomorphology, 214, 183-197.

Záruba, Q., 1922. *Study on landslide terrains in the Vsetín and Vallachian Region*. Práce z geologického ústavu čes. vys. učení technického v Praze, 170–177.

Zhou, W., Beck, B.F. & Adams, A.L., 2002. *Effective electrode array in mapping karst hazards in electrical resistivity tomography*. Environmental Geology, 42, 922–9

Received at: 10. 12. 2014
Revised at: 15. 03. 2015
Accepted for publication at: 27. 03. 2015
Published online at: 08. 04. 2015